Antiviral Research 100 (2013) 698–708

Contents lists available at ScienceDirect

Antiviral Research

journal homepage: www.elsevier.com/locate/antiviral

A novel influenza virus neuraminidase inhibitor AV5027

Alexandre V. Ivachtchenko [a,b,*], Yan A. Ivanenkov [b,c,d], Oleg D. Mitkin [b], Pavel M. Yamanushkin [b], Vadim V. Bichko [d,1], Irina A. Leneva [e], Olga V. Borisova [e]

[a] ASAVI LLC, 1835 E. Hallandale Beach Blvd, #442, Hallandale Beach, FL 33009, USA
[b] Chemical Diversity Research Institute, Rabochaya St. 2-a, 141401 Khimki, Moscow Reg., Russia
[c] The Moscow Institute of Physics and Technology, Dolgoprudny, Moskow Reg., Russia
[d] ChemDiv Inc., 6605 Nancy Ridge Drive, San Diego, CA 92121, USA
[e] Mechnikov Research Institute of Vaccines and Sera of Russian Academy of Medical Science, Moscow, Russia

ARTICLE INFO

Article history:
Received 18 July 2013
Revised 9 October 2013
Accepted 15 October 2013
Available online 24 October 2013

Keywords:
Antiviral
Neuraminidase inhibitors
Influenza
Library

ABSTRACT

A medium-sized focused library of novel Oseltamivir structural analogues with promising antiviral activity was successfully synthesized using a combinatorial approach. The synthesized compounds were then thoroughly evaluated in neuraminidase- and cell-based assays. As a result, (3*R*,4*R*,5*S*)-4-(2,2-difluoroacetylamino)-5-amino-3-(1-ethyl-propoxy)-cyclohex-1-enecarboxylic acid (AV5027) was identified as novel Hit-compound with picomolar potency. QSAR analysis was carried out based on the obtained biological data. Computational modeling was performed using a 3D-molecular docking approach and classical regression analysis. The developed integral model demonstrated a sufficient prediction accuracy and tolerance to evaluate compounds based on their potential activity against neuraminidase (NA) at least within the scaffold. Several compounds from the series can be reasonably regarded as promising anti-influenza drug-candidates.

Published by Elsevier B.V.

1. Introduction

Influenza is one of the most abundant acute respiratory diseases affecting people worldwide of all age groups and social backgrounds. Frequent seasonal epidemics lead to increased morbidity and, in more severe cases, mortality on a global scale. Annually, up to 10% among the U.S. population is affected by symptomatic influenza infection. More than 220 K persons are hospitalized and 24 K deaths due to influenza-associated illness are reported (Hayden, 2002; Monto, 2008). The highest hospitalization rate is observed of aged population, children and young persons, about one per 1 K or higher in infants, persons age 65 (approx. 20% of deaths) and older as well as persons with chronic medical conditions (Griffin, 2013). In addition to available and well-distributed anti-influenza vaccines small-molecule compounds are currently described as promising therapeutics targeted against both viral types (A and B). Influenza virus H1N1 was comprehensively described in many papers from different viewpoints (for review see: Du et al., 2010a,b; Li et al., 2011; Wang et al., 2009a,b). During the last decade, various attempts have been made to develop effective NA inhibitors with a low level of resistance (Wang et al., 2009b; Du et al., 2007; Gong et al., 2009; Wang et al., 2007, 2010; Wei et al., 2006). Oseltamivir phosphate (OsP, Fig. 1) (Kim et al., 1997), also known as Tamiflu, is one of the most effective oral neuraminidase inhibitors with a prominent antiviral activity. OsP is the pro-drug of Oseltamivir carboxylate (OsC). With respect to the route of administration, cost of production and structure optimization, the development of novel small-molecule compounds targeted against influenza is reasonably attractive. Following this concept, we have synthesized a combinatorial library of novel OsC analogues with the general structures **1a–r** (Fig. 1) (Ivachtchenko, 2012, 2013).

2. Materials and methods

2.1. Cells and viruses

Madin-Darby Canine Kidney (MDCK) cells were grown in minimal essential medium (MEM) supplemented with 10% fetal calf serum (FCS), 5 mM L-glutamine, 25 mM HEPES, 100 U/ml penicillin, 100 μg/ml streptomycin sulfate, and 100 μg/ml kanamycin sulfate, in a humidified atmosphere of 5% CO_2. The influenza virus strains A/CA/07/09 (H1N1) pdm09 and A/Duck/MN/1525/81 (H5N1) were obtained from the WHO and Utah State University (Logan, Utah, USA). Purified N1 crystals from A/Pr/8/34 (H1N1), B/Taiwan/2/62 (H1N1), A/CA/07/09 (H1N1) viruses were obtained from American Type Culture Collection (Manassas, Virginia, USA),

* Corresponding author at: Chemical Diversity Research Institute, Rabochaya St. 2-a, 141401 Khimki, Moscow Reg., Russia. Tel.: +7 495 9954941; fax: +7 495 6269780.
E-mail address: av@asavillc.com (A.V. Ivachtchenko).
[1] Tel.: +1 8587944860; fax: +1 8587944931.

0166-3542/$ - see front matter Published by Elsevier B.V.
http://dx.doi.org/10.1016/j.antiviral.2013.10.008

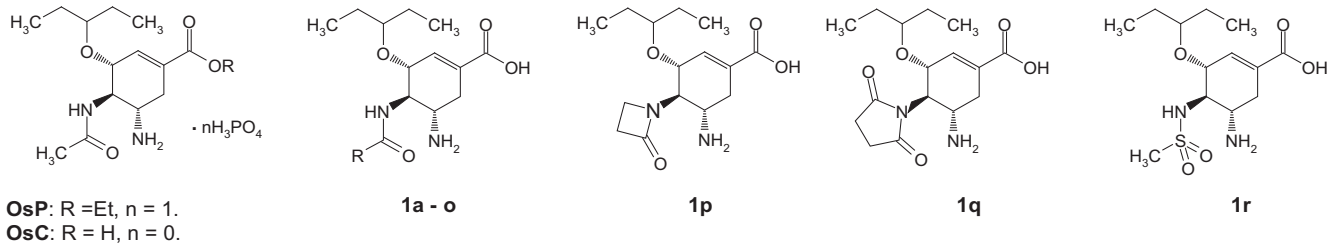

Fig. 1. OsP, OsC and compounds under investigation in this work (**1a**–**r**). **1**: R = H (**a**), CH_2=CH (**b**), CH≡C (**c**), *c*-H_7C_3 (**d**), FH_2C (**e**), F_2HC (**f**), F_3C (**g**), CF_3CH_2 (**h**), *n*- F_7C_3 (**i**), $CHF_2CF_2CF_2CF_2$ (**j**), *n*- F_9C_4 (**k**), OCH_2CH_3 (**l**), NH_2 (**m**), CH_2NH_2 (**n**), CH_2OH (**o**); R^1+R^2 = CH_2CH_2 (**p**), $CH_2CH_2C(O)$ (**q**).

and mouse-adopted A/Aichi/2/69 (H3N2) viruses were from collection of Ivanovsky Institute of Virology (Moscow, Russia).

2.2. Compounds and reagents

2.2.1. General and analytical chemistry

In all cases, the end of the reaction was determined by conversion of the substrate (LC–MS control). Evaporation of solvents from the resulting mixture and drying of the products were carried out at reduced pressure. Separation of reaction products was performed using a Shimadzu LC-8A HPLC system equipped with a Reprosil-pur C-18-AQ 10 μm 250 × 20 mm chromatographic column and Reprosil-Pur C-18-AQ 10 μm 50 × 20 mm precolumn, at a flow rate of 25 mL/min in a gradient mode with mobile phase MeCN + water + 0.05% CF3COOH.

^{1}H NMR spectra of the investigated compounds were recorded in solutions of DMSO-d_6 or CDCl3, respectively, using a Bruker DPX-400 spectrometer (400 MHz, 27 °C). LC–MS spectra were obtained using a Shimadzu LC-8A HPLC system equipped with a Waters XBridge C18 3.5 mm column (4.6 × 150 mm), PE SCIEX API 150 EX mass detection and Shimadzu spectrophotometric detector (λmax 220 and 254 nM. Purity of the synthesized compounds was determined using the LC–MS method with UV detector at the absorption wavelength of 254 nM. Purity of the compounds was more than 95%.

2.2.2. General synthetic procedure

Trifloroacetate (TFA) of OsC was prepared by basic hydrolisis of OsP, obtained from Airsea Pharmaceutical Ltd., and TFA of (3*R*,4*R*,5*S*)-4,5-diamino-3-(1-ethylpropoxy)cyclohex-1-enecarboxylic acid (**1a**) – by acidic hydrolisis of OsP. Lanamivir (LA) was obtained from AK Scientific Inc. TFAs of N(4)-substituted (3*R*,4*R*,5*S*)-4,5-diamino-3-(1-ethyl-propoxy)-cyclohex-1-enecarboxylic acids (TFA of **1a**–**r**) were synthesized starting from (3*R*,4*R*,5*S*)-4-amino-5-(Boc-amino)-3-(1-ethyl-propoxy)-cyclohex-1-enecarboxylic acid (**2a**) and its ethyl ester **2b** (Konno et al., 2008; Morita et al., 2008) according to Scheme 1.

2.2.2.1. TFA of (3R,4R,5S)-4-acetamido-5-amino-3-(1-ethylpropoxy)cyclohex-1-enecarboxylic acid (TFA of OsP). OsP (500 mg) was dissolved in 5 mL 5% lithium hydroxide solution in 1:1 dioxane–water. The resulting mixture was stirred for 1 h at room temperature. After the reaction was completed, the solvent was evaporated using a rotavapor, the residue was then treated with dioxane, filtered and rotavaped again. The resulting dry product was subjected to preparative HPLC to give TFA of OC. LC-MS (ESI) $[M+H]^+$ 285. ^{1}H NMR (DMSO-d_6) δ 12.79 (br, 1H), 8.06 (d, J = 9.6 Hz, 1H), 8.02 (br, 2H), 6.64 (s, 1H), 4.15 (m, 1H), 3.79 (q, J = 11.2 Hz, 1H), 3.39 (m, 1H), 3.28 (m, 1H), 2.74 (m, 1H), 2.31 (m, 1H), 1.88 (s, 3H), 1.42 (m, 4H), 0.83 (t, J = 7.6 Hz, 3H), 0.79 (t, J = 7.6 Hz, 3H).

2.2.2.2. TFA of (3R,4R,5S)-5-amino-3-(1-ethylpropoxy)-4-formamidocyclohex-1-enecarboxylic acid (TFA of 1a). A mixture of acid **2a** (250 mg, 0.73 mmol), formic acid (0.5 mL) and molecular sieves 3 Å (1 g) in 15 mL of toluene was refluxed for 12 h. The mixture was filtered and precipitated, then washed with ethanol and the combined filtrate was rotavaped. The resulting residue was dissolved in ethyl acetate, dried over anhydrous magnesium sulfate, filtered and rotavaped. The residue was dissolved in 3 M HCl in dioxane (3 mL) and stirred at room temperature. The reaction was monitored by TLC and LC–MS. After the reaction was completed, the mixture was rotavaped and analyzed using HPLC to give TFA of **1b** with 75% yield. LC-MS (ESI) $[M+H]^+$ 271. ^{1}H NMR (DMSO-d_6) δ 8.26 (d, J = 9.2 Hz, 1H), 8.18 (s, 1H,) 8.06 (s, 1H), 6.65 (s, 1H), 4.18 (q, J = 8 Hz, 1H), 3.86 (q, J = 10 Hz, 1H), 3.56 (s, 1H), 2.77 (m, 1H), 2.30 (m, 1H), 1.43 (m, 4H), 0.82 (m, 6H).

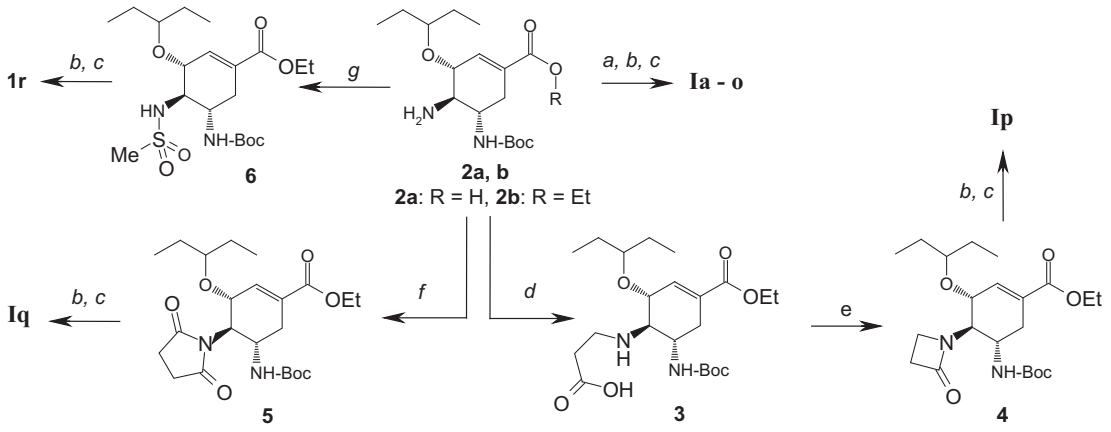

Scheme 1. The common synthetic strategy.

2.2.2.3. TFA of (3R,4R,5S)-4-acylamino-5-amino-3-(1-ethyl-propoxy)-cyclohex-1-enecarboxylic acids (TFA of 1b, d–g). General procedure. The solution of ethyl ester **2b** (1 g, 2.7 mmol), TBTU (1.3 g, 4 mmol) and appropriate carboxylic acid (4 mmol) in 10 mL DMF was stirred at 50 °C for 12 h. After the reaction was completed, the solvent was evaporated *in vacuo*, dissolved in ethyl acetate, washed with 5% aqueous potassium hydrocarbonate, dried over anhydrous magnesium sulfate, fitered and rotavaped again. The residue was subjected to preparative HPLC. The obtained intermediate compound was then dissolved in 10 mL 5% lithium hydroxide solution in 1:1 dioxane–water and stirred for 1 h at room temperature. After the hydrolisis was completed, the solvent was rotavaped, the residue was treated with dioxane, filtered and rotavaped. The resulting residue was dissolved in 30% TFA in DCM (10 mL) and stirred at room temperature. After the reaction was completed (monitoring by TLC and LC-MS), the solvent was rotavaped and the formed residue was subjected to preparative HPLC to give TFA of acids **1b**, **d**–**g** with 52–70% yield.

2.2.2.4. TFA of (3R,4R,5S)-4-acrylamido-5-amino-3-(1-ethylpropoxy)cyclohex-1-enecarboxylic acid (TFA of 1b). LC-MS (ESI) $[M+H]^+$ 297. ^{1}H NMR (DMSO-d_6) δ 8.32 (d, J = 8.8 Hz, 1H), 8.04 (s, 3H), 6.65 (s, 1H), 6.26 (m, 1H), 6.12 (m, 1H), 5.66 (d, J = 11.6 Hz, 1H), 4.19, J = 8 Hz, 1H), 3.88 (q, J = 11,2 Hz, 1H), 3.37 (m, 2H), 2.75 (m, 1H), 2.33 (m, 1H), 1.40 (m, 4H), 0.83 (t, J = 7.2 Hz, 3H), 0.71 (t, J = 7.2 Hz, 3H).

2.2.2.5. TFA of (3R,4R,5S)-5-amino-4-(cyclopropylcarbonylamino)-3-(1-ethylpropoxy) cyclohex-1-enecarboxylic acid (TFA of 1d). LC-MS (ESI) $[M+H]^+$ 311.

2.2.2.6. TFA of (3R,4R,5S)-5-amino-3-(1-ethylpropoxy)-4-(2-fluoroacetylamino) cyclohex-1-enecarboxylic acid (TFA of 1e). LC-MS (ESI) $[M+H]^+$ 303. ^{1}H NMR (DMSO-d_6) δ 9.49 (d, J = 9.2 Hz, 1H), 8.29 (s, 3H), 6.69 (s, 1H), 4.30 (d, J = 8.8 Hz, 1H), 4.17 (q, J = 5.6 Hz, 2H), 3.93 (q, J = 11.2 Hz, 1H), 3.44 (br, 1H), 3.37 (m, 1H), 2.84 (m, 1H), 2.38 (m, 1H), 1.40 (m, 4H), 1.23 (t, J = 6.8 Hz, 3H), 0.83 (t, J = 7.2 Hz, 3H), 0.75 (t, J = 7.2 Hz, 3H).

2.2.2.7. TFA of (3R,4R,5S)-5-amino-3-(1-ethylpropoxy)-4-(2,2-difluoroacetylamino)cyclohex-1-enecarboxylic acid (TFA of 1f). LC-MS (ESI) $[M+H]^+$ 321. ^{1}H NMR (DMSO-d_6) δ 12.83 (br, 1H), 8.92 (d, J = 9,2 Hz, 1H), 8.19 (s, 3H), 6.64 (s, 1H), 6.20 (t, J = 53.6 Hz, 1H), 4.27 (d, J = 8 Hz, 1H), 3.88 (m, 1H), 2.78 (m, 1H), 2.34 (m, 1H), 2.34 (m, 1H), 1.40 (m, 4H), 0.83 (t, J = 7.2 Hz, 3H), 0.76 (t, J = 7.2 Hz, 3H).

2.2.2.8. TFA of (3R,4R,5S)-5-amino-3-(1-ethylpropoxy)-4-(2,2,2-trifluoroacetylamino)cyclohex-1-enecarboxylic acid (TFA of 1g). LC-MS (ESI) $[M+H]^+$ 339. ^{1}H NMR (DMSO-d_6) δ 9.49 (d, J = 8.8 Hz, 1H), 8.30 (s, 3H), 6.65 (s, 1H), 4.29 (d, J = 8.4 Hz, 1H), 3.92 (q, J = 11.2 Hz, 2H), 3.43 (br, 1H), 3.36(m, 1H), 2.80 (m, 1H), 2.35 (m, 1H), 1.39 (m, 4H), 0.83 (t, J = 7.2 Hz, 3H), 0.75 (t, J = 7.2 Hz, 3H).

2.2.2.9. TFA of (3R,4R,5S)-5-amino-3-(1-ethylpropoxy)-4-propynoylaminocyclohex-1-enecarboxylic acid (TFA of 1c). A solution of ethyl ester **2b** (750 mg, 2 mmol), propynoic acid (213 mg, 3.04 mmol) and *N*,*N*′-dicyclohexylcarbodiimide (626 mg, 3.05 mmol) in 10 mL of DMF was stirred at ambient temperature for 12 h. After the reaction was completed, the solvent was evaporated *in vacuo*, the formed residue was treated with ether, filtered and rotavaped. The residue was dissolved in 5 mL 5% lithium hydroxide solution in 1:1 dioxane–water and stirred for 10 min at room temperature. The solvent was rotavaped, the residue was treated with dioxane, filtered and rotavaped. The residue was dissolved in 30% TFA in DCM (10 mL) and stirred at room temperature. After the reaction was completed (TLC and LC-MS), the solvent was rotavaped and the residue was subjected to preparative HPLC to give TFA of **1c**. LC-MS (ESI) $[M+H]^+$ 295. ^{1}H NMR (DMSO-d_6) δ 12.84 (br, 1H), 8.85 (d, J = 8.8 Hz, 1H), 8.12 (br, 3H), 6.62 (s, 1H), 4.26 (s, 1H), 4.17 (br, 1H), 3.84 (q, J = 11.6 Hz, 1H), 3.39 (m, 1H), 3.28 (br, 1H), 2.74 (m, 1H), 2.29 (m, 1H), 1.41 (m, 4H), 0.82 (m, 6H).

2.2.2.10. TFA of (3R,4R,5S)-5-amino-3-(1-ethylpropoxy)-4-(fluoroacylamino)cyclohex-1-enecarboxylic acids (TFA of 1h–k). General procedure. Fluorinated acylchloride (0.6 mmol) was added to the solution of ethyl ester **2b** (150 mg, 0.4 mmol) and Et_3N (113 mg, 1.22 mmol) in 1.5 mL of DCM. The resulting mixture was stirred at room temperature for 30 min. After the reaction was completed, the solvent was rotavaped, dissolved in 20 mL of ethyl acetate, washed with 5% aqueous potassium hydrocarbonate, dried over Na_2SO_4 and rotavaped. The residue was dissolved in 3 mL 5% lithium hydroxide solution in 1:1 dioxane–water and stirred for 10 min at room temperature. After the hydrolisis was completed, the solvent was rotavaped, the formed residue was treated with dioxane, filtered and rotavaped. The residue was dissolved in 3 M HCl in dioxane (3 mL) and stirred at room temperature. After the reaction was completed (TLC and LC-MS), the solvent was rotavaped and the residue was subjected to preparative HPLC to give TFA of acid **1h**–**k**.

2.2.2.11. TFA of (3R,4R,5S)-5-amino-3-(1-ethylpropoxy)-4-(3,3,3-trifluoropropionylamino)cyclohex-1-enecarboxylic acid (TFA of 1h). LC-MS (ESI) $[M+H]^+$ 367.

2.2.2.12. TFA of (3R,4R,5S)-5-amino-3-(1-ethylpropoxy)-4-(2,2,3,3,4,4,4-heptafluorobutanoylamino)-cyclohex-1-enecarboxylic acid (TFA of 1i). LC-MS (ESI) $[M+H]^+$ 439. ^{1}H NMR (DMSO-d_6) δ 9.57 (d, J = 8.8 Hz, 1H), 6.69 (s, 1H), 4.31 (br, 1H), 3.97 (q, J = 10.4 Hz, 1H), 2.81 (m, 1H), 2.34 (m, 1H), 1.48 (m, 2H), 1.31 (m, 2H), 0,81 (t, J = 7.2 Hz, 3H), 0.76 (t, J = 7.2 Hz, 3H).

2.2.2.13. TFA of (3R,4R,5S)-5-amino-3-(1-ethylpropoxy)-4-(2,2,3,3,4,4,5,5-octafluoropentanoylamino)-cyclohex-1-enecarboxylic acid (TFA of 1j). LC-MS (ESI) $[M+H]^+$ 471. ^{1}H NMR (DMSO-d_6) δ 9.47 (s, 1H), 7.06 (t, J = 48.8 Hz, 1H), 6.68 (s, 1H), 4.29 (br, 1H), 3.95 (q, J = 10.4 Hz, 1H), 2.78 (m, 1H), 2.34 (m, 1H), 1.49 (m, 2H), 1.34 (m, 2H), 0,81 (t, J = 7.2 Hz, 3H), 0.76 (t, J = 7.2 Hz, 3H).

2.2.2.14. TFA of (3R,4R,5S)-5-amino-3-(1-ethylpropoxy)-4-(2,2,3,3,4,4,5,5,5-nanofluoropentanoylamino)-cyclohex-1-enecarboxylic acid (TFA of 1k). LC-MS (ESI) $[M+H]^+$ 489. ^{1}H NMR (DMSO-d_6) δ 9.49 (s, 1H), 6.65 (s, 1H), 4.29 (br, 1H), 3.95 (q, J = 10.4 Hz, 1H), 2.80 (m, 1H), 2.35 (m, 1H), 1.49 (m, 2H), 1.33 (m, 2H), 0,81 (t, J = 7.2 Hz, 3H), 0.76 (t, J = 7.2 Hz, 3H).

2.2.2.15. TFA of (3R,4R,5S)-5-amino-3-(1-ethylpropoxy)-4-(ethyloxycarbonylamino)cyclohex-1-enecarboxylic acid (TFA of 1l). The solution of ethyl ester **2b** (300 mg, 0.81 mmol), ethyl chloroformate (114 mg, 1.2 mmol) and di-isopropylethylamine (157 mg, 1.2 mmol) in 3 mL of DCM was stirred at ambient temperature for 1 h. After the reaction was completed, the solvent was rotavaped, the residue was then treated with ether, filtered and rotavaped. The resulting residue was dissolved in 3 mL 5% lithium hydroxide solution in 1:1 dioxane–water and stirred for 10 min at room temperature. The solvent was evaporated *in vacuo* and rotavaped. The residue was treated with dioxane, filtered and rotavaped. The residue was dissolved in TFA (1 mL) and stirred at room temperature. After the reaction was completed (TLC and LC-MS), the solvent was rotavaped and the residue was subjected to preparative HPLC to give TFA of **1l**. LC-MS (ESI) $[M+H]^+$ 315.

2.2.2.16. TFA of (3R,4R,5S)-5-amino-3-(1-ethylpropoxy)-4-ureidocyclohex-1-enecarboxylic acid (TFA of 1m). KNCO (22 mg, 0.267 mmol)

was added to the solution of ethyl ester **2b** (90 mg, 0.243 mmol) in 1 mL of AcOH. The resulting mixture was stirred at ambient temperature for 1 h. After the reaction was completed, the solvent was rotavaped, stirred for 10 min with 1 mL of 5% lithium hydroxide solution and rotavaped. The residue was treated with dioxane, filtered and rotavaped. The residue was dissolved in TFA (1 mL) and stirred at room temperature. After the reaction was completed (TLC and LC-MS), the solvent was rotavaped and the residue was subjected to preparative HPLC to give TFA of **1m**. LC-MS (ESI) $[M+H]^+$ 286. ^1H NMR (DMSO-d_6) δ 7.92 (s, 3H), 6.64 (s, 1H), 6.23 (d, J = 7.6 Hz, 1H), 5.78 (br, 1H), 4.15 (m, 1H), 2.70 (m, 1H), 2.29 (m, 1H), 1.44 (m, 4H), 0.84 (m, 6H).

2.2.2.17. TFA of (3R,4R,5S)-5-amino-4-(2-aminoacetamido)-3-(1-ethylpropoxy)cyclohex-1-enecarboxylic acid (TFA of 1n). Boc-glycine (308 mg, 1.76 mmol) was added to the solution of ethyl ester **2b** (500 mg, 1.35 mmol), 1-ethyl-3-(3-dimethylaminopropyl)carbodiimide hydrochloride (387 mg, 2.03 mmol) and 1-hydroxybenzotriazole (237 mg, 1.76 mmol) in 5 mL of DMF. The reaction mixture was stirred at ambient temperature for 12 h. After the reaction was completed, the solvent was rotavaped, the residue was dissolved in ethyl acetate, washed with 5% $NaHCO_3$ solution, dried over Mg_2SO_4, rotavaped, stirred for 10 min with 5 mL of 5% lithium hydroxide solution and rotavaped. The residue was treated with dioxane, filtered and rotavaped. The residue was dissolved in TFA (1 mL) and stirred at room temperature. After the reaction was completed (TLC and LC-MS), the solvent was rotavaped and the residue was subjected to preparative HPLC to give TFA of **1n**. LC-MS (ESI) $[M+H]^+$ 300. ^1H NMR (DMSO-d_6) δ 8.68 (d, J = 8,8 Hz, 1H), 8.12 (s, 6H), 6.66 (s, 1H), 4.15 (d, J = 8 Hz, 1H), 3.86 (q, J = 11,2 Hz, 1H), 3.64 (m, 1H), 2.76 (m, 1H), 2.38 (m, 1H), 1.42 (m, 4H), 0.84 (t, J = 7.2 Hz, 3H), 0.79 (t, J = 7.2 Hz, 3H).

2.2.2.18. TFA of (3R,4R,5S)-5-amino-4-(2-hydroxyacetamido)-3-(1-ethylpropoxy)cyclohex-1-enecarboxylic acid (TFA of 1o). Glycolic acid (247 mg, 3.24 mmol) was added to the solution of ethyl ester **2b** (1 g, 2.7 mmol), di-isopropylethylamine (1.15 g, 8.92 mmol) and 1-hydroxybenzotriazole (438 mg, 3.24 mmol) in 10 mL of THF. The mixture was stirred at ambient temperature for 12 h. After the reaction was completed, the solvent was rotavaped and the residue was dissolved in ethyl acetate, washed with 5% $NaHCO_3$ solution, dried over Mg_2SO_4, rotavaped, stirred for 10 min with 5 mL of 5% lithium hydroxide solution and rotavaped. The resulting residue was treated with dioxane, filtered and rotavaped. The residue was dissolved in 3 M HCl in dioxane (3 mL) and stirred at room temperature. After the reaction was completed the solvent was rotavaped and the residue was subjected to preparative HPLC to give TFA of **1o**. LC-MS (ESI) $[M+H]^+$ 301.

2.2.2.19. TFA of (3R,4R,5S)-5-amino-3-(1-ethylpropoxy)-4-(2-oxoazetidin-1-yl)cyclohex-1-enecarboxylic acid (TFA of 1p). The solution of ethyl ester **2b** (500 mg, 1.35 mmol) and acrylic acid (485 mg, 6.75 mmol) in 10 mL of DCM was stirred at ambient temperature for 24 h. After the solvent was rotavaped the residue was subjected to preparative HPLC to give 175 mg of ethyl (3*R*,4*R*,5*S*)-5-(tert-butoxycarbonylamino)-4-(2-carboxy-ethylamino)-3-(1-ethylpropoxy)cyclohex-1-enecarboxylate (**3**), LC-MS (ESI) $[M+H]^+$ 443. Triphenylphosphine (131 mg, 0.5 mmol) and 1,2-di(pyridin-2-yl)disulfane (110 mg, 0.5 mmol) were added to the resulting solution of **3** in 40 mL of acetonitrile. The reaction mixture was then refluxed for 6 h. The mixture was rotavaped and the residue was subjected to preparative HPLC. The obtained intermediate compound **4** was dissolved in 5 mL 5% lithium hydroxide solution in 1:1 dioxane–water and stirred for 10 min at room temperature. After the hydrolisis was completed, the solvent was rotavaped, the formed residue was treated with dioxane, filtered and rotavaped. The residue was dissolved in 30% TFA in DCM (3 mL) and stirred at room temperature. After the reaction was completed, the solvent was rotavaped and the residue was subjected to preparative HPLC to give TFA of **1p**. LC-MS (ESI) [M+H]+ 297. ^1H NMR (DMSO-d_6) δ 8.25 (br, 2H), 6.67 (s, 1H), 4.40 (s, 1H), 3.56 (m, 1H), 2.81 (m, 3H).

2.2.2.20. TFA of (3R,4R,5S)-5-amino-4-(2,5-dioxopyrrolidin-1-yl)-3-(1-ethylpropoxy) cyclohex-1-enecarboxylic acid (TFA of 1q). The solution of ethyl ester **2b** (1 g, 2.7 mmol) and succinic anhydride (405 mg, 4.05 mmol) in 15 mL of pyridine was stirred at ambient temperature for 12 h. The mixture was rotavaped, dissolved in 10 mL of 5% lithium hydroxide solution in 1:1 dioxane–water and stirred for 10 min at room temperature. After the hydrolisis was completed, the solvent was rotavaped, the residue was treated with dioxane, filtered and rotavaped. The residue was dissolved in 30% TFA in DCM (7 mL) and stirred at room temperature. After the reaction was completed, the solvent was rotavaped and the residue was subjected to preparative HPLC to give TFA of **1q**. LC-MS (ESI) $[M+H]^+$ 325. ^1H NMR (DMSO-d_6) δ 6.69 (s, 1H), 4.71 (m, 1H), 4.03 (m, 2H), 2.83 (m, 1H), 2.69 (s, 4H), 2.34 (m, 1H), 1.38 (m, 2H) 1.27 (m, 2H), 0.81 (t, J = 7.2 Hz, 3H), 0.70 (t, J = 7.2 Hz, 3H).

2.2.2.21. TFA of (3R,4R,5S)-5-amino-3-(1-ethylpropoxy)-4-(methylsulfonamido)cyclohex-1-enecarboxylic acid (TFA of 1r). Methanesulfonyl chloride (170 mg, 1.49 mmol) was added to the solution of ethyl ester **2b** (500 mg, 1.35 mmol) and di-isopropylethylamine (227 mg, 1.76 mmol) in 5 mL of DCM. The solution was stirred at ambient temperature for 30 min. After the reaction was completed, the solvent was rotavaped, the residue was dissolved in ethyl acetate, washed with 5% $NaHCO_3$ solution, dried over Na_2SO_4, rotavaped, stirred for 10 min with 5 mL of 5% lithium hydroxide solution in 1:1 dioxane–water and rotavaped. The residue was treated with dioxane, filtered and rotavaped. The residue was dissolved in 3 M HCl in dioxane (3 mL) and stirred at room temperature. After the reaction was completed the solvent was rotavaped and the residue was subjected to preparative HPLC to give TFA of **1r**. LC-MS (ESI) $[M+H]^+$ 321. ^1H NMR (DMSO-d_6) δ 6.70 (s, 1H), 4.11 (m, 1H), 3.33 (br, 10H), 2.74 (m, 1H), 2.31 (m, 1H), 1.23 (br, 1H), 1.54 (br, 1H), 1.37 (m, 2H), 0.84 (m, 6H).

2.3. Molecular docking

Molecular docking (rigid simulation) was performed in ICM Pro Software (www.molsoft.com). A list of crystallographic data for various proteins isolated from influenza-type viruses is currently available within PDB collection (www.rcsb.org). For *in silico* modeling we have used the crystallographic data obtained for H1N1 influenza neuraminidase in complex with OsC (PDB code: 3TI6) (Vavricka et al., 2011). The binding mode for OsC was compared to that observed for LA (Meeprasert et al., 2012).

2.4. Regression models

A convenient prediction model was developed using two types of classical regression approaches (*linear and polynomial approximations*). The model was based on the obtained ICM-score and selected molecular descriptor calculated in Dragon software (www.talete.mi.it).

2.5. NA assay

The effect of synthesized compounds on NA activity was measured by two methods (fluorimetric and chemoluminescence assays). The fluorimetric assay was performed using the WHO protocol (Hurt, 2009). 2-(4-Methylumbelliferyl-a-D-N-acetylneu-

raminic acid sodium salt (MUNANA, Sigma, Cat. No M8639), at the final concentration of 0.1 mM, was used as a fluorescent substrate. Diluted allantoic virus containing 800–1200 fluorescence units of MUNANA was mixed with the test compound (0.01–10,000 nM) in 33 mM 2-[N-morpholino]ethanesulfonic acid (pH = 6.5) containing 4 mM $CaCl_2$ and incubated for 30 min at 37 °C. After adding the substrate and incubating at 37 °C for 1 h, the reaction was abolished by adding 0.14 M NaOH in 83% ethanol. Fluorescence was measured at an excitation wavelength of 360 nM and an emission wavelength of 448 nM. The relationship between the concentration of inhibitor and the percentage of fluorescence inhibition was determined. IC_{50} values were then calculated.

2.6. Cytotoxicity and antiviral activity of the synthesized compounds in MDCK cells infected by A/CA/07/09 (H1N1)

2.6.1. Cytotoxicity assay

Cytotoxicity of the compounds was measured using XTT (sodium 3′-[1-[(phenylamino)-carbonyl]-3,4-tetrazolium]-bis(4-methoxy-6-nitro)benzene-sulfonic acid hydrate). MDCK cells were seeded in 96-well plates at 3000 cells per well in MEM containing 10% FBS, 100 U/ml penicillin, 100 μg/ml streptomycin sulfate, and 100 μg/ml kanamycin sulfate. Cells were then incubated at 37 °C with 5% CO_2 until 90% cell confluency was reached**.** Then, MDCK cells were washed once with serum-free medium and treated with compounds at the concentrations between 1 and 1000 μg/ml or mock control solutions. Cells were grown at 37 °C and in the presence of 5% CO_2 for 72 h. Cells were washed two times and 0.1 mL XTT (1%) completely dissolved in MEM was added to the cell culture for 4 h at 37 °C in a humidified, 5% CO_2 atmosphere. The absorbance at 450 nM was read using ELISA plate reader. Cytotoxicity of the compounds was estimated by comparison of the cell treated by compounds with that of mock-treated. The value of mock-treated control cells was set as 100%.

2.6.2. Antiviral activity by ELISA

A modified enzyme-linked immunoassay (ELISA) (Belshe et al., 1988; Leneva et al., 2009) was used to measure the inhibition of virus replication by the compounds discussed. This assay represents an appropriate method to detect the expression of viral proteins in infected cells. In a brief representation, MDCK cells were seeded in 96-well plates resulted in 3000 cells per well in MEM containing 10% FBS, 100 U/ml penicillin, 100 μg/ml streptomycin sulfate, and 100 μg/ml kanamycin sulfate. Cells were then incubated at 37 °C with 5% CO_2 until 90% cell confluency was reached, then washed twice with serum-free MEM before infection. Each microliter plate included un-infected control wells, virus-infected control wells and virus-infected wells to which the compounds were added. Cells were overlaid with MEM (100 μl) containing 2.5 μg/ml N-tosyl-L-phenylalanine chloromethyl ketone (TPCK) – treated trypsin and various compounds concentrations. After incubation for 30 min at 37 °C, 100 μl of virus – containing allantoic fluid (approximately 0.1 PFU/cell) was added to all wells, except uninfected control cells. After incubation for 18 h at 37 °C in a humidified atmosphere of 5% CO_2 cells were washed and fixed by adding 50 μl of cold 0.05% glutaraldehyde in PBS. Expression of virus proteins was measured by ELISA as described previously (Belshe et al., 1988; Sugrue et al., 1990). The mouse monoclonal antibody influenza type A (CDC, WS 2208, lot 97-0068L, 10^{-3} dilution) was used. The percentage of inhibition of virus replication by the tested compounds was calculated after correction for the background (cell control) values as follows: Percent inhibition = 100 × [1−(OD_{450}) treated sample/(OD_{450}) virus control sample]. IC_{50} values (i.e., the concentration of compound required to inhibit virus replication by 50%) were determined by plotting the percentage of inhibition of virus replication as a function of compound concentration.

3. Results

3.1. In vitro NA inhibition

The ability of compounds **1a**–**r** to inhibit the NA activity of A/Pr/8/34 (H1N1), B/Taiw/2/62 (H1N1), A/Aichi/2/69 (H3N2), and A/CA/07/09 (H1N1) was evaluated following the procedure described above and compared to OsC. It was revealed that depending on the nature of the substituent at position 4 of (*3R,4R,5S*)-5-amino-3-(1-ethyl-propoxy)-cyclohex-1-enecarboxylic acids **1a**–**s** the activity of compounds (IC_{50}) range from 0.13 nM to >1000 nM (Table 1).

Antiviral activity of compounds **1c**,**d**,**g**,**h**,**o**,**p** in comparison with OsC against A/CA/07/09 (H1N1) determined using neutral red as-

Table 1
Anti-NA activity of compounds **1a**–**r** against A/Pr/8/34 (H1N1), B/Taiw/2/62 (H1N1), A/Aichi/2/69 (H3N2), and A/CA/07/09 (H1N1) influenza viruses compared to OsC and LA.[a]

Compound code/number	A/Pr/8/34 (H1N1)	B/Taiw/2/62 (H1N1)	A/Aichi/2/69 (H3N2)	A/CA/07/09 (H1N1)
	IC_{50}, nM			
OsC	0.25 ± 0.10 (7)	0.70 ± 0.18 (5)	1.11 ± 0.0710 (4)	2.33 ± 1.06 (4)
LA	nd[b]	nd	nd	0.49 ± 0.1
1a	40.0 ± 7.29 (3)	32.80 ± 5.47(3)	nd	1.43 ± 0.08
1b	0.79 ± 0.03 (2)	4.30 ± 0.90 (3)	nd	nd
1c	1.68 ± 0.52 (2)	12.90 ± 0.28 (2)	nd	nd
1d	100 ± 13 (3)	397 ± 34 (3)	nd	nd
1e	0.59 ± 0.04 (2)	0.25 ± 0.09 (3)	0.743 ± 0.568 (4)	1.00 ± 0.231 (4)
1f	0.13 ± 0.04 (5)	0.25 ± 0.08 (4)	0.598 ± 0.161 (4)	0.442 ± 0.163 (4)
1g	0.15 ± 0.03 (5)	0.65 ± 0.19 (5)	0.734 ± 0.344 (4)	0.421 ± 0.034 (4)
1h	1.18 ± 0.01(2)	4.21 ± 1.1 (2)	nd	nd
1i	871.1 ± 125 (3)	>1000 (2)	nd	nd
1j	>1000 (2)	>1000 (2)	nd	nd
1k	>1000 (2)	>1000 (2)	nd	nd
1l	>1000 (2)	>1000 (2)	nd	nd
1m	118.75 ± 11.8 (2)	67.4 ± 35.6 (2)	nd	nd
1n	343.4 ± 64 (3)	759.4 ± 110 (3)	nd	nd
1o	4.90 ± 0.03 (2)	1.57 ± 0.58 (2)	nd	nd
1p	133.3 ± 17.5 (3)	151.0 ± 11.4 (3)	nd	nd
1q	394.4 ± 9.8 (3)	>1000 (2)	nd	nd
1r	290.5 ± 61 (3)	115.4 ± 6.8 (3)	nd	nd

[a] Fluorimetric assay was used to measure influenza NA activity. Mean values are listed (2–5 experiments ± S.E.).
[b] nd – not detected.

Table 2
Comparative activity and cytotoxicity of the selected compounds in MDCK cells infected by A/CA/07/09 (H1N1).

Compound code/number	EC_{50}	CC_{50}	SI
	μM		
OsC	0.2 ± 0.08	>100	>500
1c	2.60 ± 2.28 (2)	>100	>40
1d	1.74 ± 1.09 (2)	>100	>55
1g	0.028 ± 0.025 (2)	>100	>3500
1h	0.86 ± 0.28 (3)	>100	>115
1o	22.35 ± 10.6 (3)	>100	>4.7
1p	0.62 ± 0.05 (2)	>100	>160

Table 3
Antiviral activity of (3*R*,4*R*,5*S*)-5-amino-3-(1-ethyl-propoxy)-4-(2,2-difluoro-acetyl-amino)-cyclohex-1-enecarboxylic acid TFA (**1f**), OC and LA against A/CA/07/09 (H1N1) and A/duck/MN/1525/81 (H5N1) in MDCK cells.

Compound code/number	A/CA/07/09 (H1N1)	A/Duck/MN/1525/81 (H5N1)
	EC_{50}, nM	
OsC	9.85 ± 1.98	77.4 ± 7.11
LA	15.95 ± 2.23	51.2 ± 3.76
1f	7.14 ± 1.09	23.0 ± 3.64

say in cell cultures MDCK is represented in Table 2. The comparative activity of the most effective inhibitor **1g** is shown in Table 3.

3.2. Molecular docking

Molecular docking studies (Hans-Dieter Höltje et al., 2008) can provide useful information for in-depth understanding some subtle action mechanisms at the molecular biology level, such as the marvelous allosteric mechanism revealed recently by the NMR observations on the M2 proton channel of influenza A virus (Schnell and Chou, 2008; Pielak et al., 2009; Huang et al., 2008; Due et al., 2009).

As recently described by Vavricka et al. (2011), Laninamivir binds to p09N1 with a similar active site conformation to the uncomplexed structure. Both laninamivir octanoate (CS-8958 – prodrug) and OsC binding to p09N1 induces rotation of Glu276 toward Arg224 where they form a salt bridge. This Glu276 rotation creates a hydrophobic pocket that accommodates the hydrophobic pentyl ether side chain of oseltamivir, however results in a weaker overall binding mode of laninamivir octanoate. The terminal carbon of the oseltamivir side chain is 3.73 Å from the hydrophobic Glu276 Cβ. During our modeling we observed the same perturbations within the active binding site initiated by these molecules. The computational model for the active binding site was then developed and internally tested using OC structure (2D-form without any stereo-points). The obtained result and overlapping with the template and 2D-supramolecular interfaces between active fragments of OsC and the amino acids of NA are shown in Fig. 2. We have used this model for the assessment of potential activity of compounds listed in Fig. 3.

For each structure more than ten different conformations were generated in MolSoft. All the conformations suggested were within the min of potential energy. For the assessment we have used internal "*score*" function automatically calculated in MolSoft. Score value −32 and lower is generally considered as good result – but depends on the receptor (e.g. exposed pockets or pockets with metal ions may have higher scores than −32). During the modeling we thoroughly analyzed all the scores generated. Among these values we have selected the best score assigned to the conformation that is closely related to the template interface (Figs. 2 and 3).

Direct correlation between the calculated scores and observed activities tends to 0.7 for both screening targets, while for Hits (IC_{50} < 10 nM, 8 cmpds, A/Pr/8/34 (H1N1)) this value is 0.74. Calculated scores and real activities were plotted on logarithmic scale (Fig. 4). As clearly shown in Fig. 4, the activities are all embedded appropriately raising R^2 up to 0.9. Therefore, these results allow us to speculate on a relatively good prediction power of the developed computational model. Thus, using this model, the potential number of compounds with "zero" potency against H1N1 (IC_{50} > 800 nM) can be significantly reduced or completely eliminated prior to biological trials. For instance, as depicted in Fig. 5, the estimated margin (*dotted line*) can be lined at the score point −9.00, thus, except two "outliers" (**1n** and **1r**), compounds with relatively poor activity (10 < IC_{50} < 400 nM), absolutely inactive compounds (IC_{50} > 800 nM) as well as active Hits (IC_{50} < 10 nM) forms three separate regions (*dotted boxes*). Compounds **1n** and **1r** are still needed to be *re*-tested and *re*-modeled more thoroughly to access sufficient data for their appropriate assessment.

3.3. Regression models

A convenient prediction model was then developed using two types of classical regression approaches. Thus, using Dragon software (www.talete.mi.it) more than 700 unique molecular descriptors were calculated for the compounds evaluated. Linear

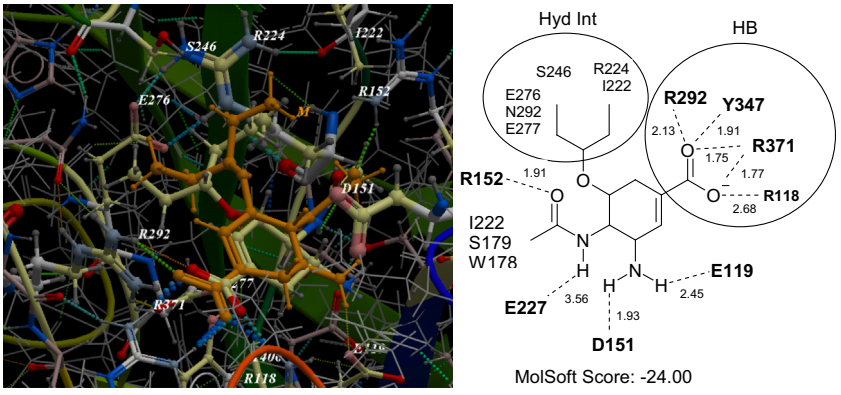

Fig. 2. OsS in the active binding site of Neuraminidase (H1N1): (a) *orange* – OsC template (*cryatallographic data*), *yellow* – the best mathed OsC conformation (RMSD: 0.09) outputed form the molecular docking; (b) 2D-supramolecular interface between the binding points of OsC and key amino acids within the active binding site of NA, where Hyd Int – hydrophobic interactions of 3-(1-ethyl-propoxy)-fragment of OsC, HB – interactions (*hydrogen bonding*) of carboxylic group of OsC with polar amino acids of NA. (For interpretation of the references to colour in this figure legend, the reader is referred to the web version of this article.)

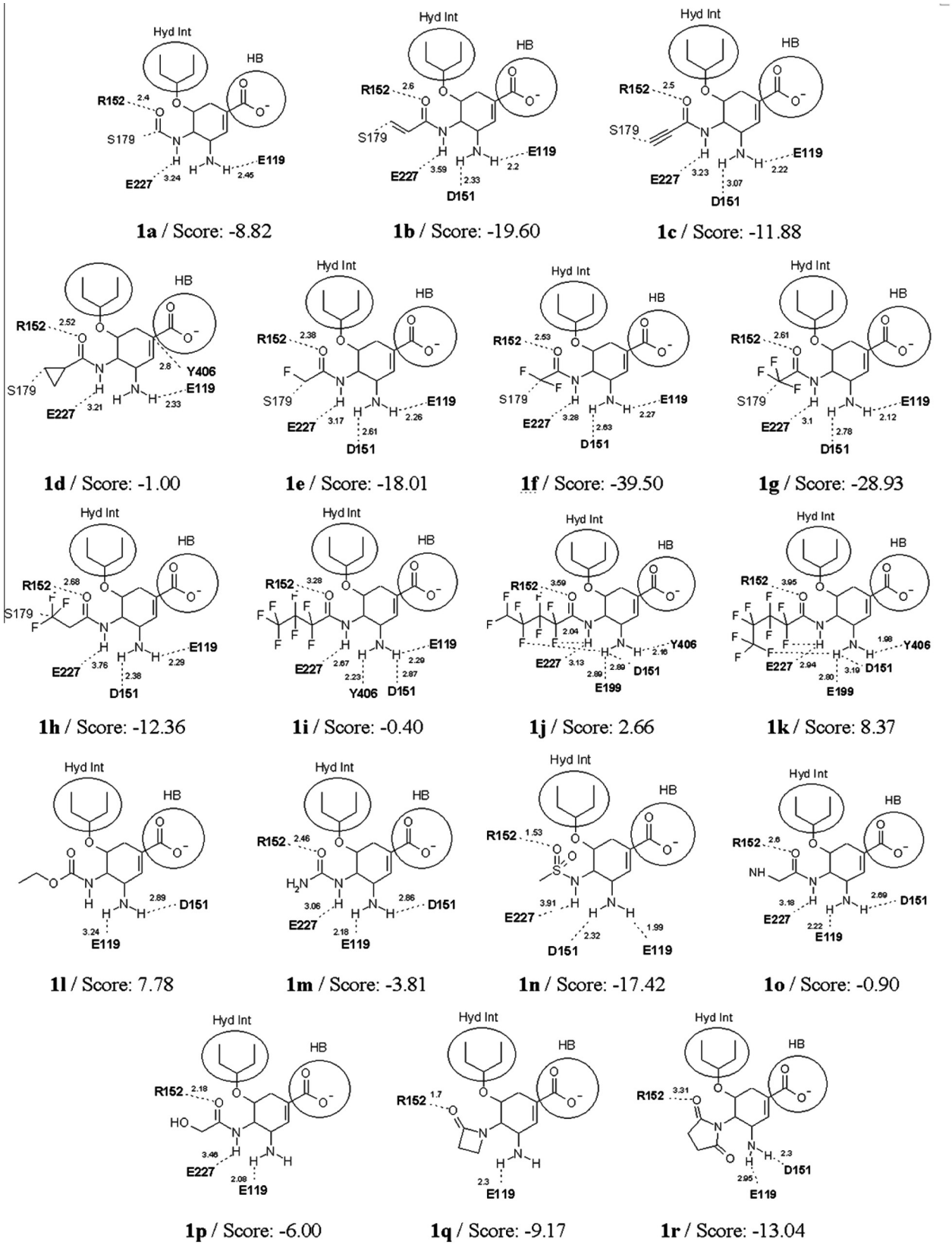

Fig. 3. The resulting supramolecular interface reconstructed based on docking results between active binding points of ligands **1a–r** and key amino acids of NA (A/CA/04/2009 (H1N1)).

correlation analysis has revealed 10 descriptors, including BELv5, H3p, MAXDP, AMR and QZZe, with *R*-value exceeded 0.60. For further regression modeling by simple linear and polynomial functions BELv5 was selected. In formal terms, BELv5 is the lowest eigenvalue n.5 of Burden matrix/weighted by atomic van der Waals volumes. The diagonal elements of Burden matrix, B*ii*, are

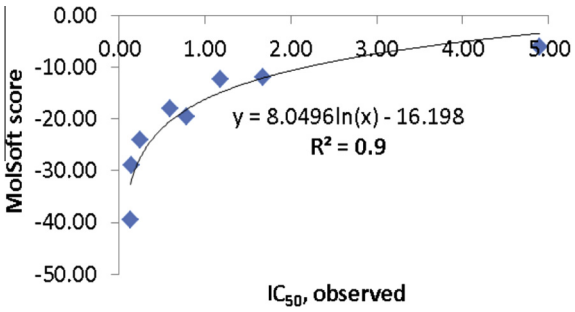

Fig. 4. Log-based approximation for Hits (IC_{50}<10 nM, 8 cmpds A/Pr/8/34 (H1N1)).

given by van der Waals volume, although other metrics are also existed, for example atomic mass, Sanderson electronegativity and polarizability of atom *i*. The element of the matrix connecting atoms *i* and *j*, B_{ij}, is equal to the square root of the bond order between atoms *i* and *j*, whereas all other elements of the matrix (corresponding non bonded atom pairs) are set to 0.001. This term can be used for the assessment of possible intermolecular van der Waals contacts within the active site of the target. It should be noted that the analogues parameter (VwInt) is automatically calculated in MolSoft software during the batch docking mode; this term is the van der Waals interaction energy. The developed models are presented in Fig. 6.

As clearly shown in Fig. 6, the best "prediction" results were achieved by polynomial regression using two descriptors (MolSoft score, BELv5) and leave-one-out procedure (LOO). Thus, squared Pearson correlation coefficient (R^2) for A/Pr/8/34 line (Fig. 6a) is relatively high – 0.89, while the analogue value for LOO cross-validation set (Q^2) is slightly less – 0.76. In statistics, the following three cross-validation methods are often used to examine a model for its effectiveness in practical application: independent dataset test, sub-sampling or K-fold cross-over test, and jackknife test (Chou and Zhang, 1995). However, of the three test methods, the jackknife test is deemed the least arbitrary that can always yield a unique result for a given benchmark dataset as elaborated in Chou (2011) and demonstrated by Eqs. (28)–(30) in Chou (2011). Accordingly, the jackknife test has been increasingly and widely used by investigators to examine the quality of various models or predictors (see, e.g.: Esmaeili et al., 2010; Georgiou et al., 2009; Zhang et al., 2008). That is why we adopted the jackknife or LOO test to validate our findings in this study.

4. Discussion

The synthesized compounds **1a**–**r** are structural analogues of OsC. The core difference is in 4-acyloylamino moiety. Therefore, the ability of the evaluated compounds to inhibit NA activity of A/Pr/8/34 (H1N1), B/Taiw/2/62 (H1N1), A/Aichi/2/69 (H3N2), and A/CA/07/09 (H1N1) was estimated in comparison with OsC. It was revealed that depending on the size and nature of the substituent at position 4, the activity of inhibitors **1a**–**r** was in the range of IC_{50}: 0.13 – (>1000) nM (see Table. 1). The best inhibition (IC_{50} = 0.13 nM to IC_{50} = 0.79 nM) was observed for 4-acryloylamino- **1b**, 4-(2-fluoroacetylamino)- **1e**, 4-(2,2-difluoroacetylamino)- **1f**, and 4-(2,2,2-trifluoroacetylamino)- **1g** derivatives against A/Pr/8/34 (H1N1) NA. It should be particularly noted that the activity of **1f** (IC_{50} = 0.13 nM) and **1g** (IC_{50} = 0.15 nM) in the performed assay is slightly higher as compared to OsC (IC_{50} = 0.25 nM). With respect to NA of B/Taiw/2/62 (H1N1), A/Aichi/2/69 (H3N2) and A/CA/07/09 (H1N1), inhibitors **1e**–**g** with IC_{50} = 0.25–1.00 nM are more active than OsC with IC_{50} = 0.70–2.33 nM as well. However, 4-(3,3,3-trifluoropropionylamino)- **1h** (IC_{50} = 1.18–4.21 nM), 4-(2-hydroxyacetylamino)- **1p** (IC_{50} = 1.57–4.90 nM) and 4-propynoylamino derivative **1c** (IC_{50} = 1.68–12.90 nM) were found to be less active against NA activity of A/Pr/8/34 (H1N1) and B/Taiw/2/62 (H1N1) as compared to the reference compound.

It was revealed that the increase in the size and branching of substituted 4-acyloylamino fragment, for instance in the case of compounds **1d**, **i**–**k**, led to a dramatic decrease in the target activity. Thus, compound **1d** showed IC_{50} = 99.79 nM (A/Pr/8/34) and IC_{50} = 397.0 nM (B/Taiw/2/62/), IC_{50} for compound **1i** was in the range of 871.1–1000 nM, nonuniformly. The incorporation of 4-formylamino group (**1a**) led to decreased activity. Derivatives **1l**, **m**, **n**, **r** exhibited poor inhibition against NA of A/Pr/8/34 (H1N1) and B/Taiw/2/62 (H1N1) with an IC_{50} value ranged from 32.8 nM

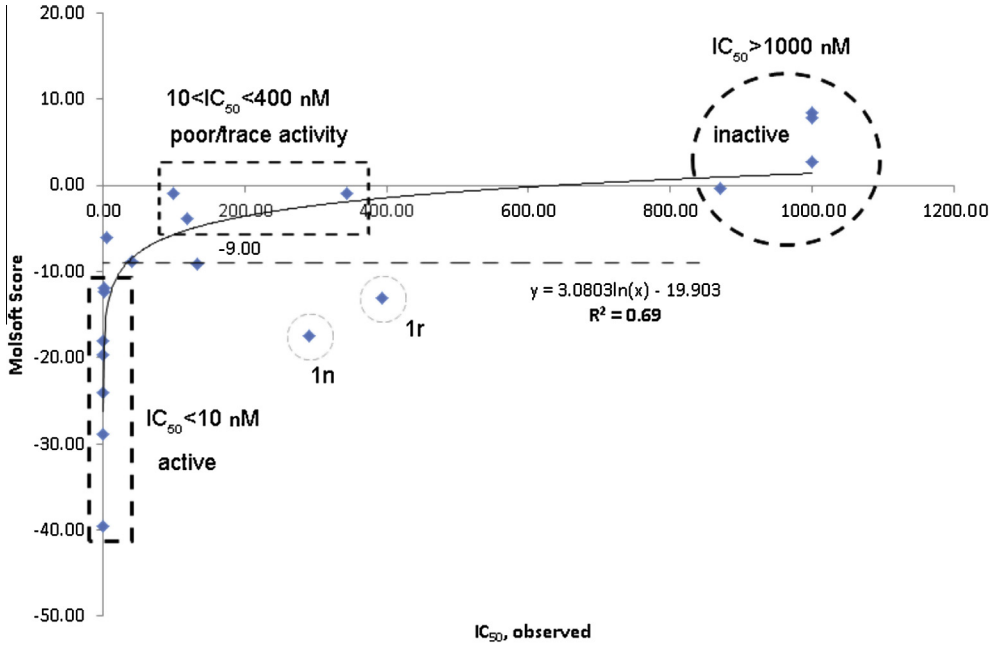

Fig. 5. Log-based approximation for all the compounds tested.

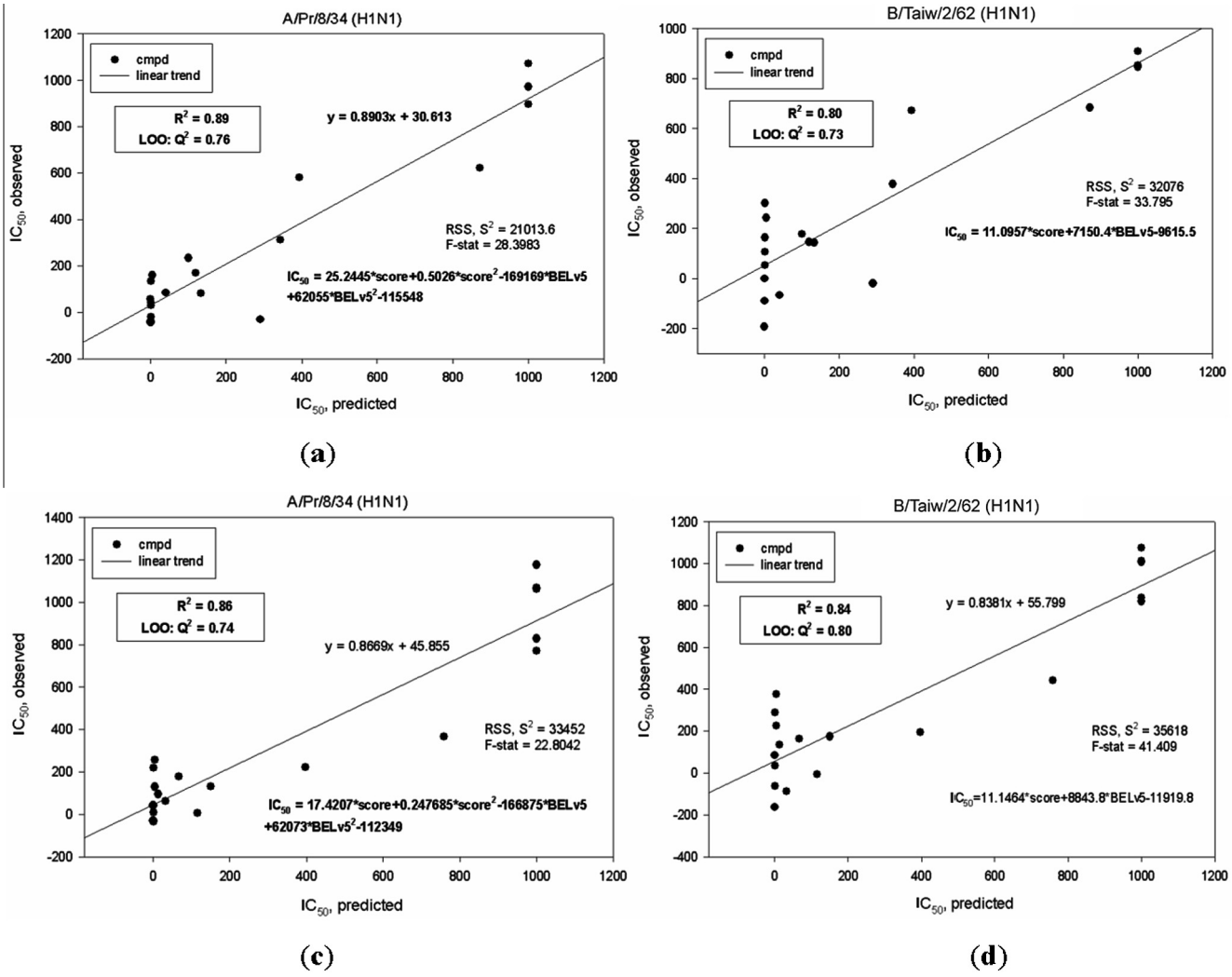

Fig. 6. Polynomial regression models (a and c) and linear approximations (b and d) for two different H1N1 lines: A/Pr/8/34 and B/Taiw/2/62. These models were developed in ChemoSoft Software [www.chemdiv.com].

for compound **1a** (B/Taiw/2/62) to >1000 nM for compound **1l** (A/Pr/8/34) and (B/Taiw/2/62). Finally, a dramatic fall in the activity was observed for 4-(2-oxo-azetidin-1-yl)- **1p** and 4-(2,5-dioxo-pyrrolidin-1-yl) derivative **1q** as compared to OsC.

The inhibition efficiency of compounds **1b**,**c**,**e**,**f**,**g**,**n**,**o** against A/CA/07/09 (H1N1) influenza virus was evaluated using NA assay and CP assay in MDCK cell culture. The resulting activity was compared to that determined for OsC (Table 2). Compound **1f** was found to be the most active NA inhibitor (IC_{50} = 0.028 μM). For example, in the same assay OsC showed 51 times less activity (IC_{50} = 1.43 μM), while for the direct analogue **1g** an IC_{50} value was 0.86 μM. Compound **1o** with IC_{50} = 0.62 μM demonstrated higher activity as compared to OsC, whereas compound **1n** was less active (IC_{50} = 22.35 μM). In addition, as shown in Table 3, the inhibition activity of Hit-compound – (3*R*,4*R*,5*S*)-5-amino-3-(1-ethyl-propoxy)-4-(2,2-difluoro-acetylamino)-cyclohex-1-enecarboxylic acid TFA (**1f**) – against NA of A/CA/07/09 (H1N1) and A/duck/MN/1525/81 (H5N1) in MDCK cells is much higher as compared to OC and LA.

Interestingly, Kim et al. (2013) have recently disclosed the novel mechanism-based anti-influenza drugs with promising anti-NA activity that function through the formation of a stabilized covalent intermediate in the influenza neuraminidase enzyme. The observation was afterwards confirmed in structural and mechanistic studies. The described compounds showed high activity in both cell-based assays and in animal models, with efficacies comparable to that observed for Zanamivir. On the bias of the study by Kim we have also suggested the covalent bonding with S179 for our compounds. However, our biological data has clearly indicated no covalent bonding with NA based on the reordered enzymatic kinetics.

Fluorine was previously described in literature as a rational bioisosteric substitution for hydrogen in CH and oxegen. It possesses high electronegativity and a small atomic radius. The C–F bond (van der Waals radius = 1.47 Å) is more nearly isosteric with the C–O bond (van der Waals radius = 1.52 Å) than with the C–H bond (van der Waals radius = 1.2 Å), but fluorine is still the smallest substituent that can be used as replacement for the C–H bond. Fluorine is more electronegative (Pauling scale) than hydrogen, 3.98 and 2.2, respectively, as well as more lipophilic. Strength C–F bonds resistant to metabolic processes, increases bioavailability and drug transport. Many examples of the effectiveness of this strategy attest to the ability of many fluorinated analogues to be recognized by protein binding sites as the natural substrate. In our case, the activity of *F*-compounds **1e**–**g** is ranged as: *nomo-F* < *di-F* = *tri-F*. The last ones were found to be almost two times more active than Os. It may be addressed to the two key features: (a) stronger

anchoring within the lipophilic pocket sustained by appropriate van der Waals contacts and (b) improved pharmacokinetic profile, especially towards membrane permeation and stability.

Given the similarity in structure between AV5027 and Os, it is expected that the Hit-compound is also likely to be sensitive towards oseltamivir-resistant NA. An extended biological trial has recently been launched to evaluate selectivity and efficiency of AV5027 against Os-resistant line. The results of this study will be reported in the next publication.

5. Conclusions

While vaccines are under development, influenza antiviral agents play crucial roles in preventing the disease progress and in controlling pandemics. However, the development of viral resistance is still the most common reason for drug failure. The resistance may drastically limit the pharmacological outcome of Oseltamivir (Li et al., 2013; Hay and Hayden, 2013). Therefore, novel small-molecule compounds particularly active against NA of influenza can be reasonably regarded as promising antiviral drugs. Thus, a medium-sized combinatorial library of direct structural analogues of OsC was readily synthesised following the approbated protocol. The obtained compounds were than thoroughly evaluated *in vitro* against NA isotypes in enzymatic and cell-based assays. As a result, novel Hit-compound – (3*R*,4*R*,5*S*)-4-(2,2-difluoroacetylamino)-5-amino-3-(1-ethyl-propoxy)-cyclohex-1-ene-carboxylic acid (**1f**, AV5027) – with picomolar activity was revealed during biological trial. Based on 3D-molecular docking approach the selected compounds were then properly scorred towards Neuraminidase (H1N1) using the crystallographic data obtained previously for OsC as a template. The calculated docking scores as well as the most significant molecular descriptor calculated in Dragon software were used to construct linear and polynomial regression models for the *in silico* assessment of IC_{50} values against the studied viral isoforms. As a result, the developed QSAR model can be readily applied for the prediction of IC_{50} values for small-molecule compounds containing the template scaffold against H1N1 neuraminidase types. The results obtained from the performed biological trials are in close correlation with the predicted activities. However, two compounds were classified incorrectly by the docking study and continuous investigation is needed to clarify this observation.

Within the follow up study we are going to present the results describing the stability and metabolism of the Hit-compound AV5027 and its close structural analogue AV5075S (ethyl-ester) as well as the efficiency of AV5075S in mice model of influenza-induced pneumonia.

Acknowledgments

The authors sincerely wish to thank Dr. I. Okun and Dr. S. Tkachenko for many valuable discussions.

References

Belshe, R.B., Smith, H.M., Hall, C.B., Betts, R., Hay, A.J., 1988. Genetic basis of resistance to rimantadine emerging during treatment of influenza virus infection. J. Virol. 62, 1508–1512.
Chou, K.C., 2011. Some remarks on protein attribute prediction and pseudo amino acid composition (50th anniversary year review). J. Theor. Biol. 273, 236–247.
Chou, K.C., Zhang, C.T., 1995. Review: prediction of protein structural classes. Crit. Rev. Biochem. Mol. Biol. 30, 275–349.
Du, Q.S., Wang, S.Q., Chou, K.C., 2007. Analogue inhibitors by modifying oseltamivir based on the crystal neuraminidase structure for treating drug-resistant H5N1 virus. Biochem. Biophys. Res. Commun. 362, 525–531.
Du, Q.S., Huang, R.B., Wang, S.Q., Chou, K.C., 2010a. Designing inhibitors of M2 proton channel against H1N1 swine influenza virus. PLoS One 5, e9388.
Du, Q.S., Wang, S.Q., Huang, R.B., Chou, K.C., 2010b. Computational 3D structures of drug-targeting proteins in the 2009–H1N1influenza A virus. Chem. Phys. Lett. 485, 191–195.
Esmaeili, M., Mohabatkar, H., Mohsenzadeh, S., 2010. Using the concept of Chou's pseudo amino acid composition for risk type prediction of human papillomaviruses. J. Theor. Biol. 263, 203–209.
Georgiou, D.N., Karakasidis, T.E., Nieto, J.J., Torres, A., 2009. Use of fuzzy clustering technique and matrices to classify amino acids and its impact to Chou's pseudo amino acid composition. J. Theor. Biol. 257, 17–26.
Gong, K., Li, L., Wang, J.F., Cheng, F., Wei, D.Q., Chou, K.C., 2009. Binding mechanism of H5N1 influenza virus neuraminidase with ligands and its implication for drug design. Med. Chem. 5, 242–249.
Griffin, M.R., 2013. Influenza vaccination: a 21st century dilemma. S. D. Med., Spec No: 110–118.
Hay, A.J., Hayden, F.G., 2013. Oseltamivir resistance during treatment of H7N9 infection. Lancet 381, 2230–2232.
Hayden, F., 2002. WHO Guidelines on the Use of Vaccines and Antivirals during Influenza – Annex 5-Considerations for the Use of Antivirals during an Influenza pandemic, Geneva, 2–4 October, Available from: <http://whqlibdoc.who.int/hq/2004/WHO_CDS_CSR_RMD_2004.8_eng.pdf>.
Höltje, H.-D., Sippl, W., Rognan, D., Folkers, G., 2008. Molecular Modeling. Wiley-VCH, Weinheim [p. 320, Revised and expanded Edition].
Huang, R.B., Du, Q.S., Wang, C.H., Chou, K.C., 2008. An in-depth analysis of the biological functional studies based on the NMR M2 channel structure of influenza A virus. Biochem. Biophys. Res. Commun. 377, 1243–1247.
Hurt, A., 2009. Standard Operating Procedure WHO – 025. WHO Collaborating Centre for Reference & Research on Influenza, Australia.
Ivachtchenko, A.V., 2012. RU 2469020.
Ivachtchenko, A.V. 2013. WO 2013/070118.
Kim, C.U., Lew, W., Williams, M.A., Liu, H., Zhang, L., Swaminathan, S., Bischofberger, N., Chen, M.S., Mendel, D.B., Tai, C.Y., Laver, W.G., Stevens, R.C., 1997. Influenza neuraminidase inhibitors possessing a novel hydrophobic interaction in the enzyme active site: design, synthesis, and structural analysis of carbocyclic sialic acid analogues with potent anti-influenza activity. J. Am. Chem. Soc. 119, 681–690.
Kim, J.H., Resende, R., Wennekes, T., Chen, H.M., Bance, N., Buchini, S., Watts, A.G., Pilling, P., Streltsov, V.A., Petric, M., Liggins, R., Barrett, S., McKimm-Breschkin, J.L., Niikura, M., Withers, S.G., 2013. Mechanism-based covalent neuraminidase inhibitors with broad-spectrum influenza antiviral activity. Science 340, 71–75.
Konno, F., Arai, T., Zhang, M.-R., Hatori, A., Yanamoto, K., Ogawa, M., Ito, G., Odawara, C., Yamasaki, T., Kato, K., Suzuki, K., 2008. Radiosyntheses of two positron emission tomography probes: [11C]Oseltamivir and its active metabolite [11C]Ro 64-0802. Bioorg. Med. Chem. Lett. 18, 1260–1263.
Leneva, I.A., Russell, R.J., Boriskin, Y.S., Hay, A.J., 2009. Characteristics of Arbidol-resistant mutants of Influenza virus: Implications for the mechanism of anti-influenza action of Arbidol. Antiviral Res. 81, 132–140.
Li, X.B., Wang, S.Q., Xu, W.R., Wang, R.L., Chou, K.C., 2011. Novel inhibitor design for Hemagglutinin against H1N1 influenza virus by core hopping method. PLoS One 6, e28111.
Li, Q., Qi, J., Wu, Y., Kiyota, H., Tanaka, K., Suhara, Y., Ohrui, H., Suzuki, Y., Vavricka, C.J., Gao, G.F., 2013. Functional and structural analysis of influenza neuraminidase N3 offers further insight into the mechanisms of oseltamivir-resistance. J. Virol. [Epub ahead of print].
Meeprasert, A., Khuntawee, W., Kamlungsua, K., Nunthaboot, N., Rungrotmongkol, T., Hannongbua, S., 2012. Binding pattern of the long acting neuraminidase inhibitor laninamivir towards influenza A subtypes H5N1 and pandemic H1N1. J. Mol. Graph. Model. 38, 148–154.
Monto, A., 2008. Viral susceptibility and the choice of influenza antivirals. Clin. Infect. Dis. 47, 346–348.
Morita, M., Sone, T., Yamatsugu, K., Solitome, Y., Matsunaga, S., Kanaia, M., Watanabe, Y., Shibasaki, M., 2008. A method for the synthesis of an oseltamivir PET tracer. Bioorg. Med. Chem. Lett. 18, 600–602.
Pielak, R.M., Jason, R., Schnell, J.R., Chou, J.J., 2009. Mechanism of drug inhibition and drug resistance of influenza A M2 channel. Proc. Natl. Acad. Sci. USA 106, 7379–7384.
Schnell, J.R., Chou, J.J., 2008. Structure and mechanism of the M2 proton channel of influenza A virus. Nature 451, 591–595.
Sugrue, R.J., Bahadur, G., Zambon, M.C., Hall-Smith, M., Douglas, A.R., Hay, A.J., 1990. Specific structural alteration of the influenza haemagglutinin by amantadine. EMBO J. 11, 3469–3476.
Vavricka, C.J., Li, Q., Wu, Y., Qi, J., Wang, M., Liu, Y., Gao, F., Liu, J., Feng, E., He, J., Wang, J., Liu, H., Jiang, H., Gao, G.F., 2011. Structural and functional analysis of laninamivir and its octanoate prodrug reveals group specific mechanisms for influenza NA inhibition. PLoS Pathog. 7, e1002249.
Wang, S.Q., Du, Q.S., Chou, K.C., 2007. Study of drug resistance of chicken influenza A virus (H5N1) from homology-modeled 3D structures of neuraminidases. Biochem. Biophys. Res. Commun. 354, 634–640.
Wang, J.F., Wei, D.Q., Chou, K.C., 2009a. Insights from investigating the interactions of adamantane-based drugs with the M2 proton channel from the H1N1 swine virus. Biochem. Biophys. Res. Commun. 388, 413–417.
Wang, S.Q., Du, Q.S., Huang, R.B., Chou, K.C., 2009b. Insights from investigating the interaction of oseltamivir (Tamiflu) with neuraminidase of the 2009 H1N1 swine flu virus. Biochem. Biophys. Res. Commun. 386, 432–436.
Wang, S.Q., Cheng, X.C., Dong, W.L., Wang, R.L., Chou, K.C., 2010. Three new powerful Oseltamivir derivatives for inhibiting the neuraminidase of influenza virus. Biochem. Biophys. Res. Commun. 401, 188–191.

Wei, D.Q., Du, Q.S., Sun, H., Chou, K.C., 2006. Insights from modeling the 3D structure of H5N1 influenza virus neuraminidase and its binding interactions with ligands. Biochem. Biophys. Res. Commun. 344, 1048–1055.

www.chemdiv.com, 2013. The official Internet site of Chemdiv – is a Fully Integrated Target-to-Clinic Contract Research Organization (CRO) headquartered in San Diego, CA USA. The company features multiple research and development (R&D) subsidiaries in Russia, Ukraine and China as well as business and logistics operations around the world.

http://www.molsoft.com, 2013. The official Internet site of Molsoft LLC, a leading provider of tools, databases and consulting services in the area of structure prediction, structural proteomics, bioinformatics, cheminformatics, molecular visualization and animation, and rational drug design.

www.rcsb.org, 2013. RCSB PDB – protein data bank.

www.talete.mi.it, 2013. The official Internet site of Talete, an Italian company working in chemometrics, data mining, experimental design, Quantitative Structure-activity Relationships (QSAR), molecular chemometrics, molecular descriptors, experimental design, multicriteria decision making and ranking methods.

Zhang, S.W., Zhang, Y.L., Yang, H.F., Zhao, C.H., Pan, Q., 2008. Using the concept of Chou's pseudo amino acid composition to predict protein subcellular localization: an approach by incorporating evolutionary information and von Neumann entropies. Amino Acids 34, 565–572.